Within-host dynamics explain patterns of antibiotic resistance in commensal bacteria

Nicholas G. Davies[1,2*], Stefan Flasche[1,2], Mark Jit[1,2,3], Katherine E. Atkins[1,2]

[1] Centre for Mathematical Modelling of Infectious Diseases, London School of Hygiene and Tropical Medicine, London WC1E 7HT, UK.

[2] Department for Infectious Disease Epidemiology, Faculty of Epidemiology and Population Health, London School of Hygiene and Tropical Medicine, London WC1E 7HT, UK.

[3] Modelling and Economics Unit, Public Health England, London SE1 8UG, UK.

* To whom correspondence should be addressed. E-mail: Nicholas.Davies@lshtm.ac.uk

The spread of antibiotic resistance, a major threat to human health, is poorly understood. Empirically, resistant strains gradually increase in prevalence as antibiotic consumption increases, but current mathematical models predict a sharp transition between full sensitivity and full resistance. In other words, we do not understand what drives persistent coexistence between resistant and sensitive strains of disease-causing bacteria in host populations. Without knowing what drives patterns of resistance, we cannot accurately predict the impact of potential strategies for managing resistance. Here, we show that within-host dynamics—bacterial growth, strain competition, and host immune responses—promote frequency-dependent selection for resistant strains, explaining patterns of resistance at the population level. By capturing these processes in a parsimonious mathematical framework, we resolve a long-standing conflict between theory and observation. Our models capture widespread coexistence for multiple bacteria-drug combinations across 30 European countries and explain associations between carriage prevalence and resistance prevalence among bacterial subtypes. A mechanistic understanding of resistance evolution is needed to accurately forecast the impact and effectiveness of resistance-management strategies.

Despite the global public health threat of antibiotic resistance[1,2], we currently lack a mechanistic understanding of how resistance spreads in human populations[3]. This gap in our knowledge is reflected in the inability of mathematical models to explain why resistance prevalence gradually increases as we move from countries with low antibiotic consumption to those with high

antibiotic consumption[3–8] (Fig. 1A). Although the mechanism driving this pattern seems intuitively obvious—greater antibiotic consumption selects for more resistance—the simplest models of disease transmission (Fig. 1B) are unable to capture the gradual rise that is observed. Instead, these models predict competitive exclusion[9]—that is, that above a particular level of antibiotic consumption, resistant strains fully outcompete sensitive strains, while below this treatment-rate threshold, they are unable to emerge at all (Fig. 1C).

This theoretical prediction stands in stark contrast to empirical patterns of widespread coexistence between sensitive and resistant strains, a trend that holds across multiple bacteria-drug combinations[6–8]. While previous work has suggested that multiple strain carriage within individuals may promote limited amounts of coexistence[3, 10], existing models cannot reproduce coexistence along the 4- to 20-fold range of treatment rates over which it is observed. Moreover, the reason why multiple carriage may promote limited coexistence is unclear. Without identifying an explicit, general mechanism for widespread coexistence, we will be unable to predict the likely impact of public health interventions for managing resistance.

Here, we show that within-host dynamics explain observed patterns of resistance in commensal bacteria. Specifically, we develop a suite of models that explicitly integrate within-host bacterial growth, strain competition, and bacterial subtype-specific host immune responses that, when calibrated to data across 30 European countries, provides a parsimonious and general explanation for empirical patterns of resistance in three commensal bacterial species, and

64 also explains patterns of resistance among competing subtypes in the
65 commensal bacterium *Streptococcus pneumoniae*.
66
67 **Results**
68
69 **Existing models fail to capture widespread coexistence.** We begin by
70 analysing a standard model of resistant disease transmission developed by
71 Lipsitch and colleagues[3, 10]. A central feature of this model is that hosts can
72 become dual carriers—that is, carriers of both sensitive and resistant strains
73 simultaneously—through sequential colonisation events (Fig. 2A). This model
74 makes two key assumptions: (1) that dual carriage is balanced, with each strain
75 carried in equal measure; and (2) that if a dual carrier is re-colonised, the
76 incoming strain "knocks out" one of the two resident strains at random.
77 Together, these assumptions preserve the crucial requirement of structural
78 neutrality at the population level[10], meaning that selection does not produce
79 coexistence "for free" by artificially promoting transmission of rare strains. In
80 this "within-host balancing" model, the amount of coexistence is governed by the
81 parameter k, the efficiency of co-colonisation relative to single colonisation.
82 While setting $k = 0$ eliminates dual carriage and recovers competitive exclusion,
83 allowing dual carriage ($0 < k \leq 1$) promotes limited coexistence (Fig. 2B). We
84 calibrated this model to European data on penicillin use and penicillin non-
85 susceptibility among *S. pneumoniae* (*Methods*). Due to the limited range of
86 coexistence predicted by the balancing model, we found that it cannot readily
87 capture observed patterns of resistance[3, 5] (Fig. 2C), even when co-colonisation is
88 more efficient than single colonisation ($k > 1$; text S2).

Although the balancing model preserves neutrality at the between-host level[10], we argue that it violates the principle of structural neutrality at the within-host level. Specifically, a structurally-neutral model should not predict that balancing selection promotes stable coexistence between two strains if the strains are biologically identical[10]. The balancing model meets this requirement at the population level[3, 10]. However, at the within-host level, when an invading strain colonises a host already carrying a larger resident strain, the balancing model implicitly assumes that the invading strain multiplies within the host—at the expense of the resident strain—until both strains are present in equal frequency, even if the two strains are biologically identical. Moreover, if a dual carrier is re-colonised, knockout immediately eliminates one of the host's existing strains, an assumption which simplifies the mathematical model but which does not have a clear mechanistic explanation. In order to preserve neutral within-host dynamics, we developed a new model that relaxes these two non-neutral assumptions.

Within-host neutrality captures widespread coexistence. In our novel "within-host neutral" model, which exhibits structural neutrality at all levels, hosts are assumed to have a fixed carrying capacity beyond which bacterial growth cannot be supported. If a host is already colonised, a new strain can invade, but rather than reaching the same frequency as the resident strain, we assume that the new strain does not increase in frequency after co-colonisation, since the host is already at carrying capacity (Fig. 2D). Strikingly, integrating within-host neutrality greatly promotes coexistence (Fig. 2E), allowing us to

114 readily capture patterns of *S. pneumoniae* resistance across European countries
115 (Fig. 2F). We originally developed this model as an individual-based simulation
116 which allows us to track arbitrary within-host strain frequencies for each host,
117 but the model can be approximated using a four-state system of differential
118 equations, which simplifies analysis and model calibration (*Methods*).
119
120 It is generally agreed that antibiotic resistance is associated with a fitness cost[11,
121 12], because in the absence of such a cost, resistant strains would fully outcompete
122 sensitive strains. We have thus far parameterised this cost by assuming that
123 resistant strains are associated with reduced transmission. Alternatively, it is
124 possible to assume that resistant strains suffer reduced within-host growth[11, 12],
125 such that a resistant strain will, in the absence of antibiotic treatment, be
126 outcompeted within the host by any sensitive strains (Fig. 2G). We captured this
127 process of within-host competition using a five-state differential equation model
128 based on our within-host neutral model (*Methods*). This addition further expands
129 the parameter space over which coexistence is maintained (Fig. 2H), improving
130 the model fit to patterns of *S. pneumoniae* penicillin non-susceptibility (Fig. 2I).
131
132 To verify the generality of our results, we re-parameterised the three models for
133 two additional facultatively-pathogenic commensal bacteria, *Escherichia coli* and
134 *Staphylococcus aureus* (*Methods*), and recalibrated the models to pan-European
135 patterns of resistance against the most widely used antibiotics for all three
136 species, which yielded a further four bacteria-drug combinations[6, 8]. Here, too,
137 the empirical data are better captured by the within-host neutral models than by
138 the balancing model (Fig. 3). Using the Akaike Information Criterion to select the

most parsimonious model, we found that the within-host competition model has the most support across all bacteria-drug combinations (Figs. 2, 3).

Within-host dynamics promotes coexistence via frequency-dependent selection. Analysis of our model reveals that frequency-dependent selection[13] is the mechanism through which within-host dynamics promote coexistence. That is, the within-host processes we have identified result in fitness advantages for either resistant or sensitive strains when those strains are rare. If resistant cells colonise a host already carrying a sensitive strain, and that host subsequently takes antibiotics, the sensitive strain is cleared and the resistant cells can grow to occupy the host's now-vacated niche; by contrast, if resistant cells colonise a host already carrying a resistant strain, antibiotic treatment has no such effect. Hence, resistant cells benefit from a fitness advantage when sensitive-strain carriers are common. Within-host competition has a complementary effect, providing sensitive cells with a fitness advantage when resistant-strain carriers are common, because sensitive cells colonising a resistant-strain carrier can grow over time to become the dominant strain in the host. Either or both of these mechanisms can promote stable coexistence by equalising the fitness of resistant and sensitive strains at intermediate carriage frequencies.

Identifying the mechanism of frequency-dependent selection helps to explain why previous model predictions for resistance prevalence are sensitive to a narrow range of antibiotic treatment rates[3, 5, 10], and hence have been unable to support coexistence over the wide range of treatment rates measured empirically. Specifically, the "balancing" and "knockout" assumptions of the

within-host balancing model create a bias against coexistence in two ways. First, balanced carriage of co-colonising strains decreases rare strains' frequency-dependent fitness benefit because it reduces the scope for rare strains to grow within dual carriers. Second, knockout reduces the prevalence of dual carriage by depleting strain diversity among hosts. Both effects reduce the strength of frequency-dependent selection for resistance, biasing models against coexistence.

Patterns of coexistence among bacterial serotypes. Many bacterial species exhibit extensive diversity in the expression of capsular proteins exposed to host immune systems, which subdivides species into several distinct "serotypes" that, like resistant versus sensitive strains, are known to stably coexist in host populations[14, 15]. Host immune memory can promote coexistence between serotypes, because more common serotypes are more likely to provoke a host immune response owing to previous exposure, creating frequency-dependent selection for serotype diversity[14, 15]. However, similar considerations to those detailed above reveal that serotype diversity can also be promoted through a related mechanism that does not require host immune memory. In our within-host neutral model, coexistence is promoted by resistant strains multiplying to take the place of co-colonising sensitive strains that are cleared by antibiotic treatment. A similar mechanism might promote stable coexistence between commensal bacteria serotypes, so long as—when co-colonising a host—serotypes can be independently cleared by a host immune response, with any strains of the same serotype being cleared simultaneously. This would result in a

188 fitness advantage for a strain co-colonising a host carrying a different serotype,
189 promoting serotype diversity even in the absence of immune memory.
190
191 To test this hypothesis, we extended our individual-based model to track
192 coexistence between five serotypes differing in their clearance rate, their
193 transmission rate or their within-host growth rate. We found that independent
194 clearance of serotypes from co-colonised hosts can promote stable coexistence
195 between serotypes, even when serotypes exhibit intrinsic fitness differences
196 (Fig. 4A). Unlike in previous models which have not explicitly tracked within-
197 host dynamics[14, 15], we find that acquired immunity is not needed to maintain
198 limited amounts of serotype diversity. Moreover, we found that resistance
199 prevalence varied across coexisting serotypes, with the direction of the trend in
200 resistance prevalence among serotypes depending on whether the cost of
201 resistance was parameterised as a transmission-rate cost or a growth-rate cost.
202 When resistance is associated with a transmission-rate cost, resistance is more
203 strongly selected in fitter serotypes, whether serotypes differ in fitness due to
204 differences in duration of carriage[4], transmissibility, or within-host growth (Fig.
205 4B). This reflects an empirical association between serotype fitness and
206 resistance prevalence observed in *S. pneumoniae*[4]. By contrast, when resistance
207 is associated with a within-host growth-rate cost (Fig. 4C), resistance is more
208 strongly selected in less-fit serotypes (Fig. 4D). Thus, our model would predict
209 that the association between resistance prevalence and serotype fitness may
210 depend on the balance between these two putative costs of resistance.
211

212 **Resistance prevalence among pneumococcal serotypes.** Finally, we used this
213 proof of principle to evaluate carriage distribution and resistance prevalence in a
214 model with 30 co-circulating *S. pneumoniae* serotypes parameterised with
215 observed differences in duration of carriage. We found that independent
216 clearance of serotypes alone was insufficient to support the high diversity of
217 pneumococcal serotype carriage observed in human populations, with only five
218 serotypes maintained (text S4). However, introducing serotype-specific
219 immunity[14] to our within-host neutral framework was sufficient to capture much
220 of the observed pneumococcal diversity and patterns of resistance among
221 pneumococcal serotypes (Fig. 5).
222

223 **Discussion**
224

225 We have proposed a novel, parsimonious and pathogen-independent
226 mathematical framework that, unlike previous models, captures empirical
227 patterns of antibiotic resistance across countries differing in treatment rates and
228 among serotypes. We argue that frequency-dependent selection drives these
229 patterns of resistance and that coexistence of sensitive and resistant strains is
230 promoted by integrating structural neutrality at the within-host level.
231 Frequency-dependent selection has long been known to promote stable
232 coexistence among animal, plant, and bacterial competitors[16–19], and we show
233 here that it could also have a pivotal role in maintaining coexistence between
234 sensitive and resistant strains of commensal bacteria.
235

Although a number of alternative mechanisms that could explain coexistence between drug-sensitive and resistant pathogens have been proposed[3–5, 20–23], some support only modest amounts of coexistence[3, 5], while other proposed mechanisms may be difficult to generalize empirically, such as strongly age-assortative mixing[4], independent mappings of balancing selection[4], or specific immune responses to resistance-associated phenotypes[3, 21–23]. Our framework of within-host neutrality provides two advances on previous work: it harmonises pathogen dynamics occurring at the between-host and within-host levels, and it allows us to better and more parsimoniously capture observed patterns of resistance prevalence across a range of important bacteria-drug combinations.

Dual carriage of resistant and sensitive strains, a crucial factor for coexistence, is generated in our models via sequential colonisation. The empirical prevalence of dual carriage is not well known, but a study of *S. aureus* carriage in children found 21% of hosts carried both resistant and sensitive strains[24] and—although resistance phenotypes were not measured—other studies have found up to 48% multiple carriage of genetically-distinct *S. pneumoniae* strains[25, 26] and 42% multiple carriage of virulent *E. coli* strains[27]. These studies find that carriage is typically dominated by one strain with other strains carried at low frequency, consistent with our model's carrying-capacity assumptions. Dual carriage could also occur through *de novo* mutation, which is likely to be especially important for long-lived chronic infections such as colonisations of the cystic fibrosis lung by *Pseudomonas aeruginosa*[28, 29]. While it is possible that coexistence is maintained by forces additional to dual carriage, we suggest that any model

incorporating dual carriage should observe within-host neutrality to avoid biasing against coexistence.

Antibiotic resistance is one of the foremost threats to human health, and combating this threat will require the global deployment of coordinated interventions[1, 2]. Mathematical models of disease transmission will play a crucial role in this endeavour, because they can explicitly integrate the mechanisms that drive resistance evolution in a population-level framework and allow us to quantify long-term trends as well as the likely impact of any large-scale interventions for reducing resistance[30]. Providing a framework in which to answer public health questions will require a balance between mathematical tractability and identifiability of the models on one side, and necessary complexity on the other; building on the simple models proposed here will help to establish that balance. If mathematical models are able to incorporate a truly mechanistic understanding of resistance, they will be better able to explain common patterns of resistance and to accurately predict the effect of interventions at a national and global level[30]. With growing calls for an integrated and multifaceted approach to the problem of antimicrobial resistance[1, 2], a new generation of mechanistic mathematical models will be uniquely placed to support the evidence-based adoption of impactful and cost-effective strategies.

References and Notes

1. World Health Organization (2016) *United Nations high-level meeting on antimicrobial resistance.* http://www.who.int/antimicrobial-resistance/events/UNGA-meeting-amr-sept2016/en.

2. O'Neill J, *ed*. (2016) *Tackling drug-resistant infections globally: final report and recommendations*. https://amr-review.org/home.html.

3. Colijn C, *et al.* (2010) What is the mechanism for persistent coexistence of drug-susceptible and drug-resistant strains of *Streptococcus pneumoniae*? *J. R. Soc. Interface* **7**, 905–919.

4. Lehtinen S, *et al.* (2017) Evolution of antibiotic resistance is linked to any genetic mechanism affecting bacterial duration of carriage. *Proc Natl Acad Sci USA* **114**, 1075–1080.

5. Cobey S, *et al.* (2017) Host population structure and treatment frequency maintain balancing selection on drug resistance. *J R Soc Interface* **14**, 20170295.

6. European Centre for Disease Prevention and Control. (2017) Antimicrobial consumption rates by country. http://ecdc.europa.eu/en/healthtopics/antimicrobial-resistance-and-consumption/antimicrobial-consumption/esac-net-database/Pages/Antimicrobial-consumption-rates-by-country.aspx.

7. European Antimicrobial Resistance Surveillance System (2007) *EARSS Annual Report 2007*. Bilthoven: EARSS.

8. European Centre for Disease Prevention and Control (2017) *Antimicrobial resistance surveillance in Europe 2015. Annual Report of the European*

Antimicrobial Resistance Surveillance Network (EARS-Net). Stockholm: ECDC.

9. Hardin G (1960) The competitive exclusion principle. *Science* **131**, 1292–1297.
10. Lipsitch M, Colijn C, Cohen T, Hanage WP, Fraser C (2009) No coexistence for free: neutral null models for multistrain pathogens. *Epidemics* **1**, 2–13.
11. Andersson DI (2006) The biological cost of mutational antibiotic resistance: any practical conclusions? *Curr Opin Microbiol* **9**, 461–465.
12. Andersson DI, Hughes D (2010) Antibiotic resistance and its cost: is it possible to reverse resistance? *Nat Rev Microbiol* **8**, 260–271.
13. Ayala FJ, Campbell CA (1974) Frequency-dependent selection. *Ann Rev Ecol Syst* **5**, 115–138.
14. Cobey S, Lipsitch M. (2012) Niche and neutral effects of acquired immunity permit coexistence of pneumococcal serotypes. *Science* **335**, 1376–1380.
15. Flasche S, *et al.* (2013) The impact of specific and non-specific immunity on the ecology of *Streptococcus pneumoniae* and the implications for vaccination. *Proc R Soc B* **280**, 20131939.
16. Ayala FJ (1971) Competition between species: frequency dependence. *Science* **171**, 820–824.
17. Sinervo B, Lively CM (1996) The rock-paper-scissors game and the evolution of alternative male strategies. *Nature* **380**, 240–243.
18. Gigord LDB, Macnair MR, Smithson A (2001) Negative frequency-dependent selection maintains a dramatic flower color polymorphism in the rewardless orchid *Dactylorhiza sambucina* (L.) Soò. *Proc Natl Acad Sci USA* **98**, 6253–6255.

19. Rainey PB, Travisano M (1998) Adaptive radiation in a heterogeneous environment. *Nature* **394**, 69–72.

20. Austin DJ, Kristinsson KG, Anderson RM (1999) The relationship between the volume of antimicrobial consumption in human communities and the frequency of resistance. *Proc Natl Acad Sci USA* **96**, 1152–1156.

21. Dietz K (1979) Epidemiologic interference of virus populations. *J Math Biol* **8**, 291–300.

22. Gupta S, Swinton J, Anderson RM (1994) Theoretical studies of the effects of heterogeneity in the parasite population on the transmission dynamics of malaria. *Proc R Soc Lond B* **256**, 231–238.

23. Lipsitch M (1997) Vaccination against colonizing bacteria with multiple serotypes. *Proc Natl Acad Sci USA* **94**, 6571–6576.

24. Mongkolrattanothai K, *et al* (2011) Simultaneous carriage of multiple genotypes of *Staphylococcus aureus* in children. *J Med Microbiol* **60**, 317–322.

25. Kamng'ona AW, *et al.* (2015) High multiple carriage and emergence of *Streptococcus pneumoniae* vaccine serotype variants in Malawian children. *BMC Inf Diseases* **15**, 234.

26. Turner P, *et al.* (2011) Improved detection of nasopharyngeal cocolonization by multiple pneumococcal serotypes by use of latex agglutination or molecular serotyping by microarray. *J Clin Microbiol* **49**, 1784–1789.

27. Martinez-Medina M, *et al.* (2009) Molecular diversity of *Escherichia coli* in the human gut: new ecological evidence supporting the role of adherent-invasive *E. coli* (AIEC) in Crohn's disease. *Inflamm Bowel Dis* **15**, 872–882.

354 28. Smith EE, *et al.* (2006) Genetic adaptation by *Pseudomonas aeruginosa* to the
355 airways of cystic fibrosis patients. *Proc Natl Acad Sci USA* **103**, 8487–
356 8492.
357 29. Yang L, *et al.* (2011) Evolutionary dynamics of bacteria in a human host
358 environment. *Proc Natl Acad Sci USA* **108**, 7481–7486.
359 30. Atkins KE, *et al.* Use of mathematical modelling to assess the impact of
360 vaccines on antibiotic resistance. *Lancet Infect Dis*, in press.
361 31. Chewapreecha C, *et al.* (2014) Dense genomic sampling identifies highways
362 of pneumococcal recombination. *Nat Genet* **46**, 305–309.
363 32. Bogaert D, *et al.* (2004) Colonisation by *Streptococcus pneumoniae* and
364 *Staphylococcus aureus* in healthy children. *Lancet* **363**, 1871–1872.
365 33. Goossens MC, Catry B, Verhaegen J (2013) Antimicrobial resistance to
366 benzylpenicillin in invasive pneumococcal disease in Belgium, 2003–
367 2010: the effect of altering clinical breakpoints. *Epidemiol Infect* **141**,
368 490–495.
369 34. Ter Braak CJF (2006) A Markov chain Monte Carlo version of the genetic
370 algorithm differential evolution: easy Bayesian computing for real
371 parameter spaces. *Stat Comp* **16**, 239–249.
372 35. Nelder JA, Mead R (1965) A simplex method for function minimization. *Comp*
373 *J* **7**, 308–313.
374 36. Li B, *et al.* (2012) Duration of stool colonization in healthy medical students
375 with extended-spectrum-β-lactamase-producing *Escherichia coli*.
376 *Antimicrob Agents Chemother* **56**, 4558–4559.

377 37. Apisarnthanarak A, Bailey TC, Fraser VJ (2008) Duration of stool colonization
378 in patients infected with extended-spectrum β-lactamase-producing
379 *Escherichia coli* and *Klebsiella pneumoniae*. *Clin Infect Dis* **46**, 1322–1333.
380 38. Shenoy ES, Paras ML, Noubary F, Walensky RP, Hooper DC (2014) Natural
381 history of colonization with methicillin-resistant *Staphylococcus aureus*
382 (MRSA) and vancomycin-resistant *Enterococcus* (VRE): a systematic
383 review. *BMC Infect Dis* **14**, 177.
384 39. Larsson AK, *et al.* (2011) Duration of methicillin-resistant *Staphylococcus*
385 *aureus* colonization after diagnosis: A four-year experience from southern
386 Sweden. *Scand J Inf Dis* **43**, 456–462.
387 40. Martinez-Medina M, *et al.* (2009) Molecular diversity of *Escherichia coli* in the
388 human gut: new ecological evidence supporting the role of adherent-
389 invasive *E. coli* (AIEC) in Crohn's disease. *Inflamm Bowel Dis* **15**, 872–882.
390 41. European Centre for Disease Prevention and Control (2014) *Surveillance of*
391 *antimicrobial consumption in Europe 2011*. Stockholm: ECDC.
392 <https://ecdc.europa.eu/sites/portal/files/media/en/publications/Publi
393 cations/antimicrobial-consumption-europe-surveillance-2011.pdf>.

394

395 **Acknowledgements:** We thank M. Davies for assistance. NGD, MJ and KEA were
396 funded by the National Institute for Health Research Health Protection Research
397 Unit (NIHR HPRU) in Immunisation at the London School of Hygiene and
398 Tropical Medicine in partnership with Public Health England (PHE). The views
399 expressed are those of the authors and not necessarily those of the NHS, the
400 NIHR, the Department of Health or PHE. The authors declare no competing

401 financial interests. NGD, SF, MJ and KEA conceived the study; NGD performed the

402 analyses; NGD and KEA drafted the manuscript, which all authors revised.

403

404 **Supplementary Materials**

405 Materials and Methods

406 Tables S1–S2

407 Figs S1–S13

408 References (32 – 41)

409 **Figures**

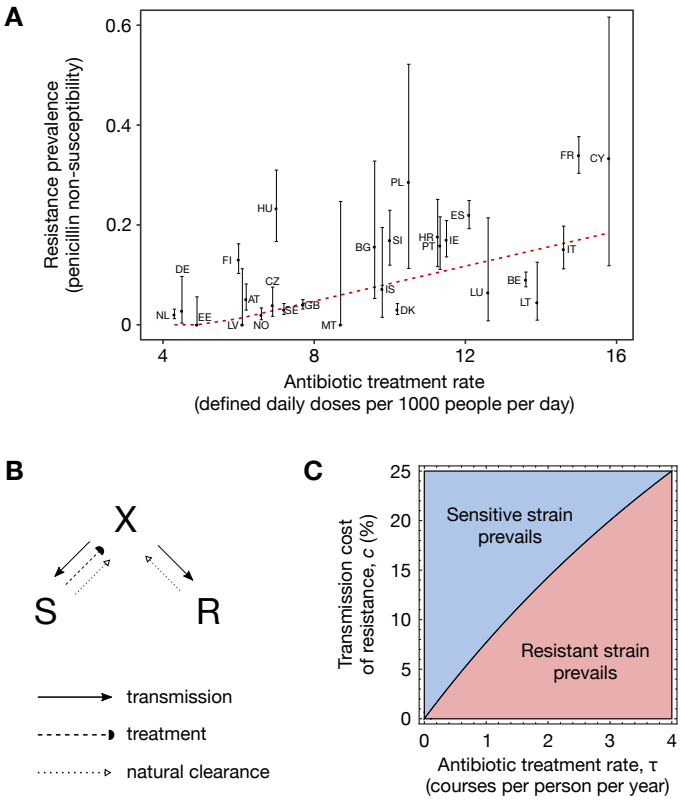

410

411 **Fig. 1.** The problem of coexistence. **(A)** The prevalence of penicillin non-

412 susceptibility in invasive isolates of *S. pneumoniae* across 27 European countries

413 illustrates widespread coexistence. This pattern of gradual increase of resistance

414 with the antibiotic treatment rate holds across many pathogen-drug

415 combinations[6–8]. **(B)** A simple two-strain single-carriage model defined by the

416 system of ordinary differential equations $\frac{dS}{dt} = \beta SX - (u + \tau)S, \frac{dR}{dt} = \beta(1 -$

417 $c)RX - uR, X = 1 - S - R$, with X non-carriers, S sensitive-strain carriers, and R

418 resistant-strain carriers. Here, β is the rate of transmission (solid arrows), τ is

419 the rate of antibiotic treatment (dashed arrow), u is the rate of natural clearance

420 (dotted arrows), and c is the transmission cost of resistance. **(C)** Contrary to

421 observed patterns of coexistence, the single-carriage model predicts competitive

422 exclusion, with the sensitive strain dominating the resistant strain if $\tau > cu/(1-c)$;

423 here, $\beta = 4$ months^{-1}, $u = 1$ months^{-1}.

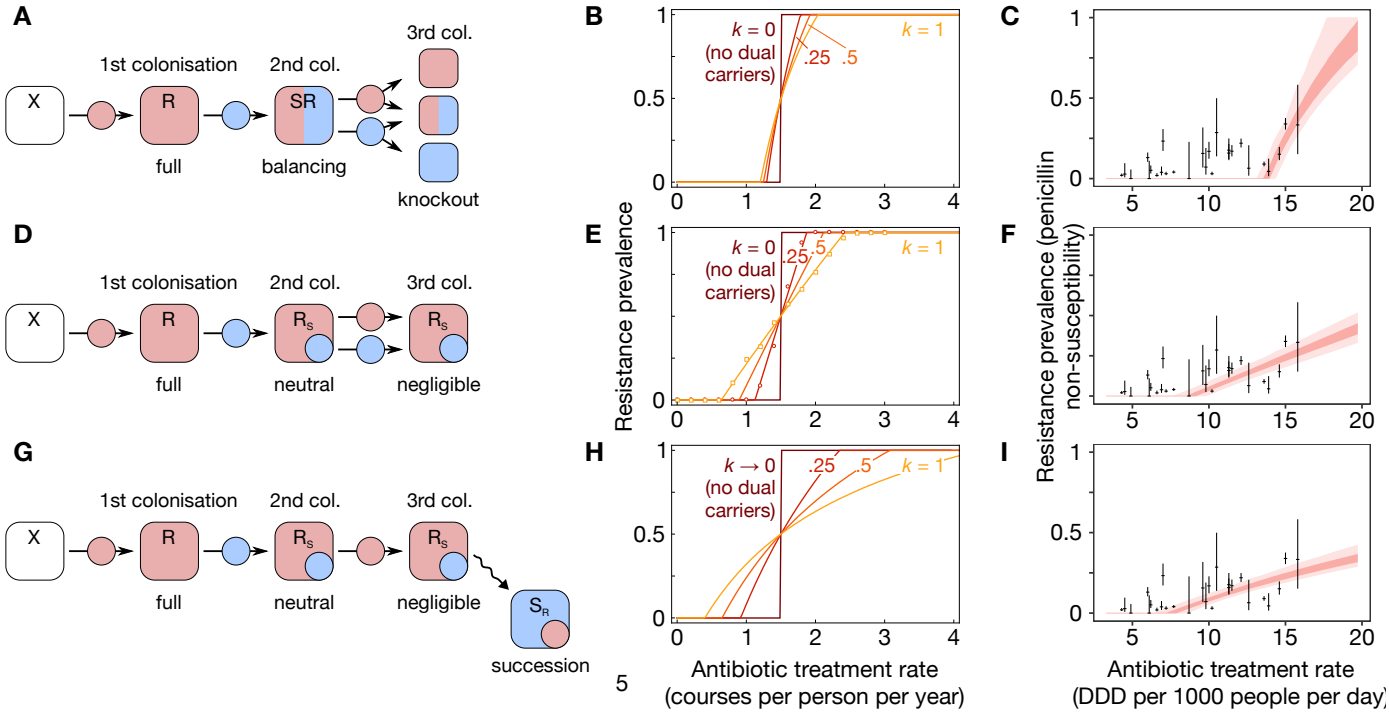

Fig. 2. Three models of dual carriage. **(A)** The within-host balancing model[10] extends the single-carriage model (Fig. 1B) by permitting simultaneous dual carriage. An example sequence of colonisation events illustrates equal co-colonisation and knockout. **(B)** Although coexistence increases with the efficiency of multiple carriage, *k*, the region of coexistence remains small for the within-host balancing model. **(C)** When calibrated to penicillin non-susceptibility in *S. pneumoniae* across European countries, the balancing model does not capture widespread coexistence. **(D)** The same example sequence of colonisation events as in panel **A** illustrates the absence of the balancing and knockout mechanisms in the within-host neutral model. **(E)** Integrating within-host neutrality expands the region of coexistence. Overlaid markers are results from our individual-based model with no limit to the number of co-colonisation states (see Methods). **(F)** Within-host neutrality yields a better fit to empirical data. **(G)** The same example sequence illustrates frequency-dependent selection acting on

439 the sensitive strain when within-host competition is added to the within-host
440 neutral model. **(H)** Within-host competition further increases coexistence and **(I)**
441 the resulting model provides the best fit to the data (relative likelihood of 1.0 for
442 the within-host competition model, 0.635 for the within-host neutral model, and
443 4.49×10^{-5} for the balancing model).

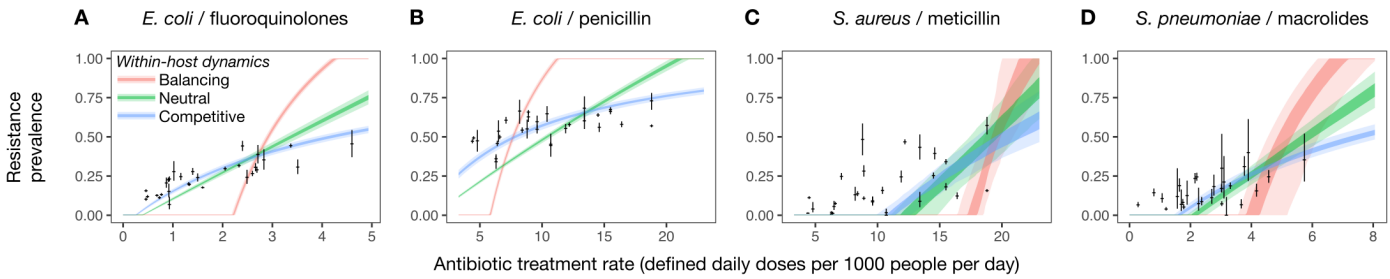

444

445 **Fig. 3.** Within-host dynamics explain patterns of resistance across commensal

446 bacteria. Within-host neutral models with (blue) or without (green) within-host

447 competition capture persistent coexistence, while the balancing model (red)

448 does not. Compared with the within-host neutral model with strain competition,

449 the relative likelihood of the balancing and neutral models are, respectively, **(A)**

450 2.45×10^{-127}, and 3.85×10^{-15}; **(B)** 3.22×10^{-163} and 3.41×10^{-28}; **(C)** 6.33×10^{-4} and

451 0.141; and **(D)** 6.57×10^{-15} and 2.28×10^{-3}.

452

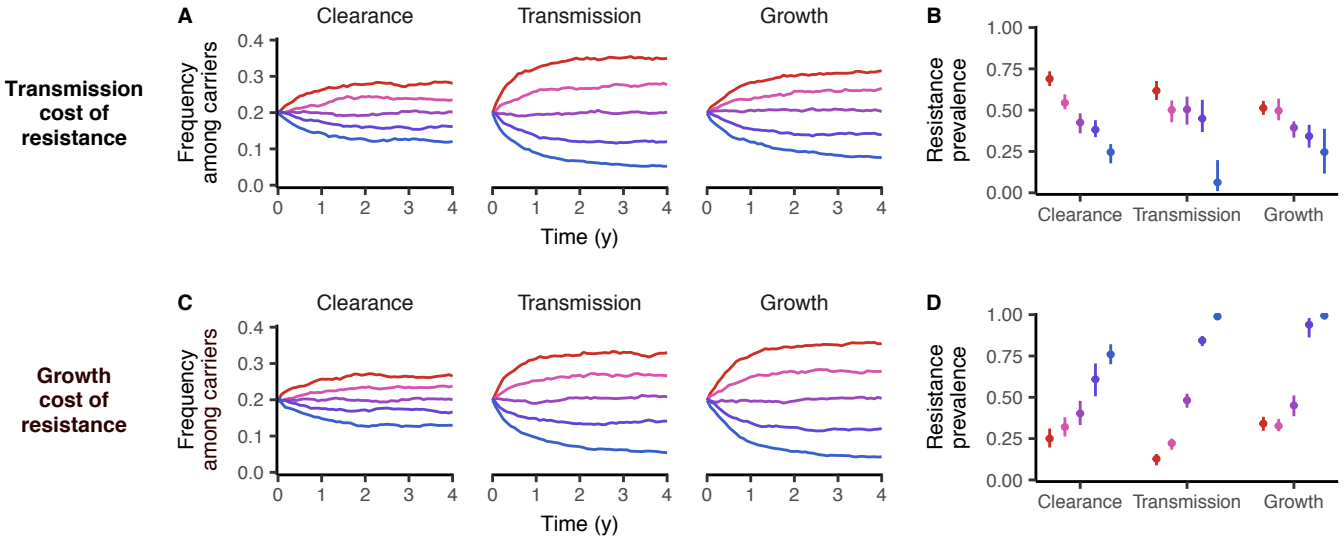

Fig. 4. Within-host dynamics promote coexistence between serotypes, and intrinsic fitness differences between serotypes are correlated with resistance prevalence within serotypes. **(A)** In a model with five serotypes differing in various measures of intrinsic fitness, independent clearance of serotypes from hosts supports limited coexistence between serotypes even in the absence of immune memory. **(B)** When resistance carries a transmission-rate cost, fitter serotypes are more strongly selected for resistance. **(C, D)** When resistance carries a growth-rate cost, fitter serotypes are less strongly selected for resistance. Serotypes are assumed to differ in clearance rate (u = 0.96, 0.98, 1.0, 1.02, 1.04), transmission rate (β = 2.2, 2.1, 2.0, 1.9, 1.9), or within-host growth rates (growth rate penalties α = 0, 0.015, 0.03, 0.045, 0.06; see Methods). In each plot, the fittest serotype is shown in red. The mean and 95% interquantile range for the last 50 years of the 100-year simulation is shown. Resistance is assumed to be associated with either a 10% transmission-rate cost (A, B) or a growth-rate penalty of 0.025 (C, D).

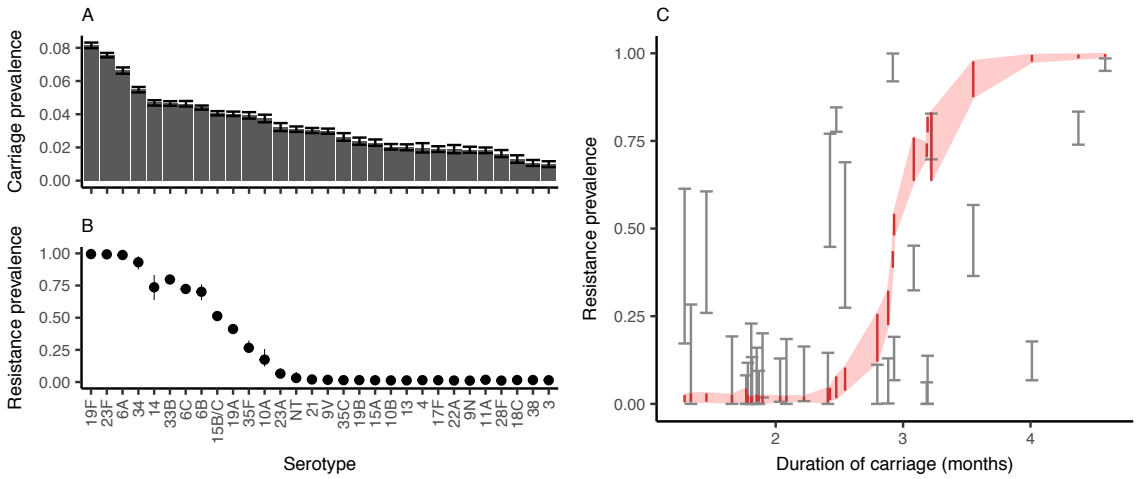

Fig. 5. Resistance prevalence among pneumococcal serotypes. **(A)** We parameterised our individual-based within-host neutral model to simulate a population in which 30 common pneumococcal serotypes circulate, using a previously-published data set[4, 31] to assign measured durations of carriage to each serotype. Serotypes are otherwise undifferentiated and we assume no within-host competition. Incorporating a simple model of host immune memory (see *Methods*) recovers extensive diversity in **(A)** pneumococcal carriage and **(B)** resistance prevalence. **(C)** The positive relationship between duration of carriage and resistance prevalence observed empirically (black error bars, showing 95% confidence intervals for duration of carriage) is recovered in the model (red ribbon, showing 95% interquantile range for each serotype in the final 50 years of the 100-year simulation).

Materials and Methods

Systems of ordinary differential equations

In the main text, we discuss four epidemiological models of antibiotic resistance: a single-carriage model, and three multiple-carriage models (the within-host balancing model, the within-host neutral model, and the within-host competition model). These models can be analysed using the systems of differential equations presented in this section, or using an alternative stochastic individual-based model formulation which is presented below (see *Individual-based model*). The ordinary differential equation models can simulate two strains at a time (sensitive and resistant), and are used for exposition of the key principles and for model calibration (Figs. 1–3). The individual-based models can simulate an arbitrary number of strains, and are used for validation of the ordinary differential equation models (Fig. 2) and for analysing serotype dynamics (Figs. 4 and 5).

Single-carriage model — The single-carriage model is given by

$$\frac{dS}{dt} = \beta SX - (u+\tau)S$$

$$\frac{dR}{dt} = \beta(1-c)RX - uR$$

$$X = 1 - S - R\,. \qquad (1)$$

Here, $S = S(t)$ is the fraction of sensitive strain carriers in the population; $R = R(t)$ is the fraction of resistant strain carriers in the population; and $X = X(t)$ is the fraction of non-carriers. The parameter β is the person-to-person transmission rate of the sensitive strain, u is the natural clearance rate, τ is the per capita rate of antibiotic treatment, and c is the transmission cost of resistance. Here, the resistance prevalence is $\rho = R/(1-X)$.

Within-host balancing model — Following previous work[3, 10], the balancing model is given by

$$\frac{dS}{dt} = \beta S_{tot} X - (u+\tau)S - k\beta(1-c)R_{tot}S + \frac{k\beta S_{tot}D}{2}$$

$$\frac{dR}{dt} = \beta(1-c)RX - uR - k\beta S_{tot}R + \frac{k\beta(1-c)R_{tot}D}{2} + \tau D$$

$$\frac{dD}{dt} = k\beta(1-c)R_{tot}S + k\beta S_{tot}R - (u+\tau)D - k\beta S_{tot}D - k\beta(1-c)R_{tot}D$$

$$X = 1 - S - R - D\,. \qquad (2)$$

Here, the additional compartment $D = D(t)$ is the fraction of dual carriers in the population (*SR* carriers in Fig. 2A of the main text), k is the efficiency of multiple colonisation relative to single colonisation, and $S_{tot} = S + D/2$ and $R_{tot} = R + D/2$ give the effective population burden of sensitive- and resistant-strain colonisation, respectively. The resistance prevalence is $\rho = R_{tot}/(1-X)$.

Within-host neutrality model — The novel neutral model is given by

$$\frac{dS}{dt} = \beta(S + S_R)X - (u+\tau)S - k\beta RS$$

$$\frac{dR}{dt} = \beta(1-c)RX - uR + \tau S_R$$

$$\frac{dS_R}{dt} = k\beta(1-c)RS - (u+\tau)S_R$$

$$X = 1 - S - R - S_R \,. \qquad (3)$$

Here, the compartment $S_R = S_R(t)$ captures the fraction of the population predominantly colonised with sensitive bacteria, but also carrying a small amount of resistant bacteria that are carried in insufficient quantity to transmit, and $S + S_R$ gives the effective population burden of sensitive-strain colonisation. The corresponding R_S compartment is omitted as it does not impact upon the overall resistance prevalence in this model, $\rho = R/(1-X)$; however, for tracking the overall prevalence of dual carriers (both S_R and R_S), the full neutral model can be recovered from equations 4 below by setting $b = 0$.

Within-host competition model — The neutral model with within-host competition is given by

$$\frac{dS}{dt} = \beta(S + S_R)X - (u+\tau)S - k\beta(R + R_S)S$$

$$\frac{dR}{dt} = \beta RX - uR + \tau(S_R + R_S) - k\beta(S + S_R)R$$

$$\frac{dS_R}{dt} = k\beta(R + R_S)S - (u+\tau)S_R + bR_S$$

$$\frac{dR_S}{dt} = k\beta(S + S_R)R - (u+\tau)R_S - bR_S$$

$$X = 1 - S - R - S_R - R_S \,. \qquad (4)$$

552 Here, the R_S compartment captures dual carriers predominantly colonised with
553 resistant bacteria plus a small amount of sensitive bacteria, and b captures the
554 within-host benefit of sensitivity, *i.e.* the rate at which R_S carriers become S_R
555 carriers. The resistance prevalence is $\rho = (R + R_S)/(1-X)$.
556
557 *Ordinary differential equation solutions* — All models are solved by setting single-
558 carriage compartments (S and R) equal to 0.001 and all dual-carriage
559 compartments to 0, then integrating the systems of ordinary differential
560 equations numerically in C++ using the Runge–Kutta Dorman–Prince method
561 until they reach equilibrium.
562
563 Individual-based model
564
565 The individual-based model follows the same logic as the ordinary differential
566 equation models, except it can simulate more than two strains simultaneously
567 and within-host dynamics are simulated more explicitly.
568
569 In the individual-based model, hosts are indexed by $i \in 1 \ldots N$, where N is the
570 population size, and there are M strains indexed by $j \in 1 \ldots M$. Each host is
571 characterised by a vector $(f_{i,1}, f_{i,2}, \ldots, f_{i,M})$ giving the load of each strain colonising
572 the host, where $0 \leq f_{i,j} \leq 1$ for all i, j and the host's total bacterial load is $f_i = \Sigma_j f_{i,j}$.
573 The force of infection of strain $_j$ is $\lambda_j = (\beta/N) \Sigma_i q_i (1-c_j) f_{i,j}$, where β is the basic
574 transmission rate, c_j is the transmission cost associated with strain j, $q_i = 0$ if $f_i =$
575 0, and $q_i = 1/f_i$ if $f_i > 0$; that is, hosts with no bacterial load are not infectious, but
576 all hosts with any nonzero bacterial load are assumed to be equally infectious,

aside from differences in the transmission cost associated with each of their carried strains. Henceforth, we omit host subscripts *i* to focus on a single host.

The model proceeds in discrete time steps. Each time step, hosts may or may not experience a series of "events" (colonisation, treatment, or natural clearance) and then their strain carriage is "updated" according to a series of rules. For a time step Δt, an event which occurs at rate r over the whole population is assumed to occur to each host with probability $r\Delta t$. Colonisation events occur at rate λ_j for each strain j if a host is uncolonised and rate $k\lambda_j$ if a host is already colonised. When a host is colonised by strain j, the host's carriage of that strain is increased by the "germ size" ι, where $\iota << 1$, so we have $f_j' = f_j + \iota$, *i.e.* colonisation by strain j increases the host's carriage of that strain by ι while leaving carriage of other strains unaffected. Additionally, hosts are colonised by importation of strains at a low rate $\omega = 1\text{x}10^{-5}$ to prevent stochastic elimination of strains at low carriage frequencies[14]. Treatment events occur at rate τ. When a host undergoes treatment, the host's carriage of each strain becomes $f_j' = Q_j f_j$ for all j, where $Q_j = 0$ for sensitive strains and $Q_j = 1$ for resistant strains, *i.e.* all sensitive strains are set to zero frequency. Clearance events occur at rate u_s for each serotype s; each strain j is associated with a serotype s_j, and there may be more than one strain with the same serotype. When a host undergoes natural clearance, the host's carriage of each strain becomes $f_j' = 0$ for all j for which $s_j = s$, *i.e.* carriage of all strains of serotype s are set to zero while carriage of other strains is unaffected.

Once all "events" for a time step have been done, each host is "updated" according to the following rules. Under the within-host neutral model, total strain carriage for colonised hosts is always maintained at the carrying capacity of the host (*i.e.* $f = \Sigma f_j = 1$). Specifically, a host's bacterial load becomes $f_j' = f_j/f$ for all j. Under the within-host competition model, strain dynamics are modelled using an ordinary differential equation model of logistic growth and cell death; that is, we integrate from time t to time $t + \Delta t$ the differential equations defined by

$$\frac{df_j}{dt} = f_j(\mu(1-\alpha_j)\left(1-\frac{f}{K}\right)-\nu) \qquad (5)$$

for all strains j, where μ is the basic growth rate, α_j is the growth-rate penalty for strain j, K is the host density regulation constant, and ν is the cell death rate. For all simulations of the within-host competition model, we assume μ = 200, ν = 100, and $K = 2$, which maintains total strain carriage for each host at $f = 1$ when no strain has a growth-rate penalty. The model proceeds in discrete time steps of $\Delta t = 0.001$ or $\Delta t = 0.005$ months.

Host immune memory

When modelling the full range of pneumococcal serotypes (Fig. 5), we simulate host immune memory as follows. A host who has previously cleared a strain of serotype s (*i.e.* through natural clearance only, not treatment) cannot be re-infected by that serotype. However, hosts are randomly cleared of their immune

memory at rate $1/a_{\max}$, where $a_{\max}$ is the maximum host age simulated in the model, which approximates new hosts entering the population at birth at the same rate that hosts leave the population due to aging. We assume $a_{\max}$ = 60 months, reflecting the relative importance of pneumococcal transmission in hosts aged 5 years or under[3, 32].

Model parameterisation and calibration

We calibrated the models using European Centre for Disease Prevention and Control data on penicillin consumption[6] and the prevalence of penicillin non-susceptibility among *S. pneumoniae* invasive isolates[7] from 2007 for 27 European countries. We focused on the year 2007 for this data set as criteria for penicillin non-susceptibility in *S. pneumoniae* were changed in some countries after this year, yielding inconsistencies in resistance data between countries[3, 33]. For calibration to all other bacteria-drug combinations, we used data for the same 27 countries collected in 2015, the most recent year for which data are available[6, 8]. Antibiotic consumption rates were given in defined daily doses (DDD) per thousand people; we converted these to overall treatment rates by assuming that 10 DDD comprise one treatment course for penicillin[4] and fluoroquinolones, while 7 DDD comprise one treatment course for macrolides.

We used Markov chain Monte Carlo with differential evolution[34] to calibrate the model output to empirical data. We assumed that the number of resistant isolates tested in a given country follows a binomial distribution with success probability drawn from a beta distribution, with the model-predicted resistance

prevalence as the mode of the beta distribution. Setting the success probability as a random variable allowed us to account for between-country variation in resistance prevalence not captured by our dynamic model. The likelihood of the observed resistance prevalence for bacteria-antibiotic set *j* across all countries, $\boldsymbol{d_j}$, given the model predicted resistance prevalence, ρ_j, and prevalence of carriage, Y_j, is

$$L_j(\boldsymbol{d_j}|\rho_j, \boldsymbol{Y_j}) =$$

$$\prod_{i=1}^{C_j}\left(\left[Y_j^{(0)} \le Y(\tau_{i,j}) \le Y_j^{(1)}\right]\int_{x=0}^{1}\mathrm{Beta}\left(x\middle|\omega=\rho_j(\tau_{i,j}),\kappa=\kappa_j^*\right)\mathrm{Bin}\left(r_{i,j}\middle|n_{i,j},x\right)dx\right).$$

Here, $\left[Y_j^{(0)} \le Y(\tau_{i,j}) \le Y_j^{(1)}\right]$ is 1 if $Y(\tau_{i,j})$ lies between $Y_j^{(0)}$ and $Y_j^{(1)}$, which are the lower and upper bounds of duration of carriage, respectively, and 0 otherwise; $\mathrm{Beta}(x|\omega,\kappa) = x^{\alpha-1}(1-x)^{\beta-1}\Gamma(\alpha+\beta)/(\Gamma(\alpha)\Gamma(\beta))|_{\alpha=\omega(\kappa-2)+1,\ \beta=(1-\omega)(\kappa-2)+1}$ is the beta distribution probability density with mode ω and concentration κ; and $\mathrm{Bin}(r|n,x) = \binom{n}{r}x^r(1-x)^{n-r}$ is the binomial distribution probability density. There are C_j countries in the data set *j* labelled $i = 1 \ldots C_j$; for a country *i* and bacteria-antibiotic set *j*, the measured antibiotic use is $\tau_{i,j}$, the number of samples taken of a particular bacteria is $n_{i,j}$, and the number of those samples tested as non-susceptible to the particular antibiotic is $r_{i,j}$. The model prediction for resistance prevalence given treatment rate τ is $\rho_j(\tau)$, the model prediction for prevalence of carriage given treatment rate τ is $Y_j(\tau)$, and the estimated concentration around the best-fit line, estimated from the data, is κ_j^*.

To estimate the concentration κ_j^* from the resistance prevalence data, we used a truncated line function $f(\tau) = \max(0, a + g\tau)$ as the modal antibiotic resistance prevalence and fixed κ_j^* as the concentration. We calculated the maximum likelihood estimates of a_j^*, g_j^*, and κ_j^* by using the Nelder-Mead algorithm[35] to maximize the following likelihood function:

$$L_j^{(1)}(a_j^*, g_j^*, \kappa_j^*)$$

$$= \prod_{i=1}^{c_j} \int_{x=0}^{1} \mathrm{Beta}\left(x \middle| \omega = \max\left(0, a_j^* \tau_{i,j} + g_j^*\right), \kappa = \kappa_j^*\right) \mathrm{Bin}\left(r_{i,j} \middle| n_{i,j}, x\right) dx$$

Priors for all model fitting were identified from the literature and were bacteria-specific (see below).

For illustrative purposes, the parameters *c* and *b* for Fig. 2B, E, H were chosen such that τ = 1.5 courses per person per year would lead to 50% resistance prevalence. This τ was chosen to roughly coincide with *S. pneumoniae* empirical data[6, 8]. Other parameters used were β = 4, u = 1 (ref. 3) and *k* as given in the figure.

Priors for duration of carriage

For *S. pneumoniae*, we assume an average duration of carriage of 1 month (ref. 3), giving a clearance rate u = 1 months^{-1}. For *E. coli*, we assume that the average

691 duration of carriage is 59 to 98 days[36, 37], and accordingly set a uniform prior for
692 u over the range 0.3–0.5 months^{-1}. For *S. aureus*, we assume a duration of
693 carriage of 3.3 months (estimated from ambulatory patients clearing MRSA[38]) to
694 5.9 months (ref. 39), and accordingly set a uniform prior for u over the range
695 0.17–0.3 months^{-1}.
696
697 The transmission parameter, β, is constrained by the likelihood function (see
698 below), so we set a uniform prior on β wide enough to overlap the full range of
699 observed carriage prevalence, Y, given the range of clearance rates u and
700 treatment rates τ (*i.e.* $Y = 1 - (u + \tau)/\beta$ for the sensitive strain alone, and $Y = 1 -$
701 $u/(\beta(1-c))$ for the resistant strain alone). Specifically, for *S. pneumoniae*, we use
702 the range 1–6; for *E. coli*, we use the range 1–10; and for *S. aureus*, we use the
703 range 0.1–2.
704
705 *Likelihood ranges for carriage prevalence*
706
707 In the main text, we detail how the likelihood function used in model fitting
708 constrains model output such that all countries must exhibit a prevalence of
709 carriage Y such that $Y^{(0)} \leq Y \leq Y^{(1)}$. For *S. pneumoniae*, we follow Colijn *et al.*[3] in
710 assuming $0.2 \leq Y \leq 0.8$ in children. For *E. coli*, we restrict our attention to
711 extraintestinal pathogenic *E. coli* (ExPEC), a subset of *E. coli* that is responsible
712 for most invasive infections, and assume $0.499 \leq Y \leq 0.942$, which is derived from
713 95% confidence intervals around the observed prevalence of carriage of ExPEC
714 (9 of 12 healthy control subjects) from Martinez-Medina *et al.*[40]. Finally, for *S.*
715 *aureus*, we adopt $0.2 \leq Y \leq 0.6$ based on Bogaert *et al.*[32], which is based on the

observed range of *S. aureus* colonization in Dutch children, with a slightly wider range to capture more variation between European countries.

MCMC details

Following the differential evolution MCMC algorithm[34], we run 10*n* chains, where *n* is the number of free parameters in the model, *i.e.* 30 for *S. pneumoniae* (for which carriage duration is fixed at 1 month) and 40 for *E. coli* and *S. aureus*, for which carriage duration is not fixed. The burn-in period lasts 1,000 iterations, after which 100,000 samples from the posterior are taken across all chains.

Sources for antibiotic consumption and resistance prevalence data

We used data from the European Centre for Disease Prevention and Control (ECDC) and from the European Antimicrobial Resistance Surveillance Network (EARS-Net) to parameterize our models for the consumption of antibiotics and prevalence of antibiotic resistance in EU countries.

The ECDC provides information on antimicrobial consumption in defined daily doses (DDD) per 1000 inhabitants per day for participating countries, with antimicrobials broken down into categories as classified in the World Health Organisation's (WHO) Anatomical Therapeutic Chemical (ATC) Classification System. Consumption is classified into primary care and hospital use, with the majority of use in primary care. We focus on primary care usage only, as hospital

741 usage data is sparse and we are focusing on community-acquired bacterial
742 carriage. The ECDC releases online publications summarizing consumption data
743 (*e.g.* ref. 41) and maintains a queryable online database[6].
744
745 EARS-Net, formerly EARSS, provides information on resistance levels as
746 measured in invasive isolates of various bacterial pathogens isolated from blood
747 and cerebrospinal fluid[7, 8]. We assume that invasive isolates are a sample of
748 commensally-carried strains[4]. We summarize the data used and sources for the
749 five data sets analysed (**Table S1**).

Data set	Consumption: *ATC code, sector, year, and source*	Resistance: *Pathogen, resistance metric, year, and source*
Streptococcus pneumoniae penicillin resistance, 2007 (Figs. 1–2, main text)	J01C (Beta-lactam antibacterials, penicillins), primary care, 2007 (ECDC 2017b, 2014†)	*S. pneumoniae*, percentage non-susceptible to penicillin, 2007 (EARSS 2007)
Escherichia coli fluoroquinolone resistance, 2015 (Fig. 3a, main text)	J01MA (Fluoroquinolones), primary care, 2015 (ECDC 2017b)	*E. coli*, percentage resistant to fluoroquinolones, 2015 (ECDC 2017a)
E. coli penicillin resistance, 2015 (Fig. 3b, main text)	J01C (Beta-lactam antibacterials, penicillins), primary care, 2015 (ECDC 2017b)	*E. coli*, percentage resistant to aminopenicillins, 2015 (ECDC 2017a)
Staphylococcus aureus meticillin resistance, 2015 (Fig. 3c, main text)	J01C (Beta-lactam antibacterials, penicillins), primary care, 2015 (ECDC 2017b)	*S. aureus*, percentage resistant to meticillin (MRSA), 2015 (ECDC 2017a)
S. pneumoniae macrolide resistance, 2015 (Fig. 3d, main text)	J01FA (Macrolides), primary care, 2015 (ECDC 2017b)	*S. pneumoniae*, percentage non-susceptible to macrolides, 2015 (ECDC 2017a)

Table S1. Data sources for antibiotic consumption and antimicrobial resistance across five pathogen-drug combinations. †Portugal recorded no penicillin consumption for 2007 in the online ECDC database[6], but the 2011 ECDC report[41] provides the corrected figure of 11.3 DDD per 1000 inhabitants per day for 2007.

Supporting information

S1. Posterior distributions from model fitting

Here, we show the posterior distributions from model fitting from the main analysis (**Fig. S1–S5**).

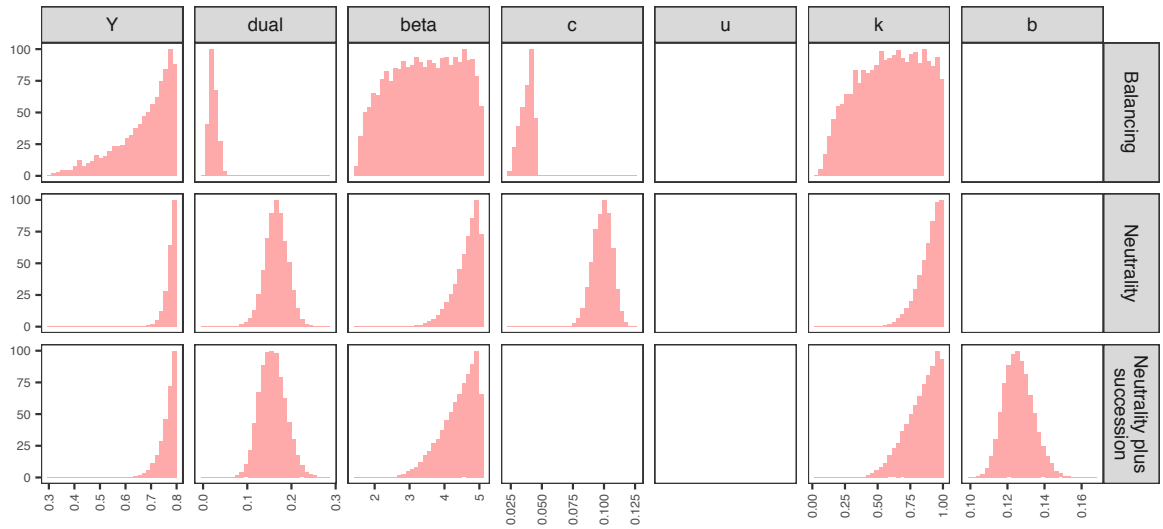

Figure S1 | Posterior distribution for *S. pneumoniae* / penicillin, 2007. *Y* gives the overall prevalence of carriage (whether single or dual) in the population; *dual* gives the fraction of carriers who carry both sensitive and resistant strains; *beta* gives the transmission parameter; *c* gives the transmission cost of resistance; *u* gives the clearance rate (if the clearance rate is subject to fitting; for *S. pneumoniae*, *u* = 1); *k* gives the efficiency of recolonisation, and *b* gives the within-host rate of succession (see *Methods*, main text, for details).

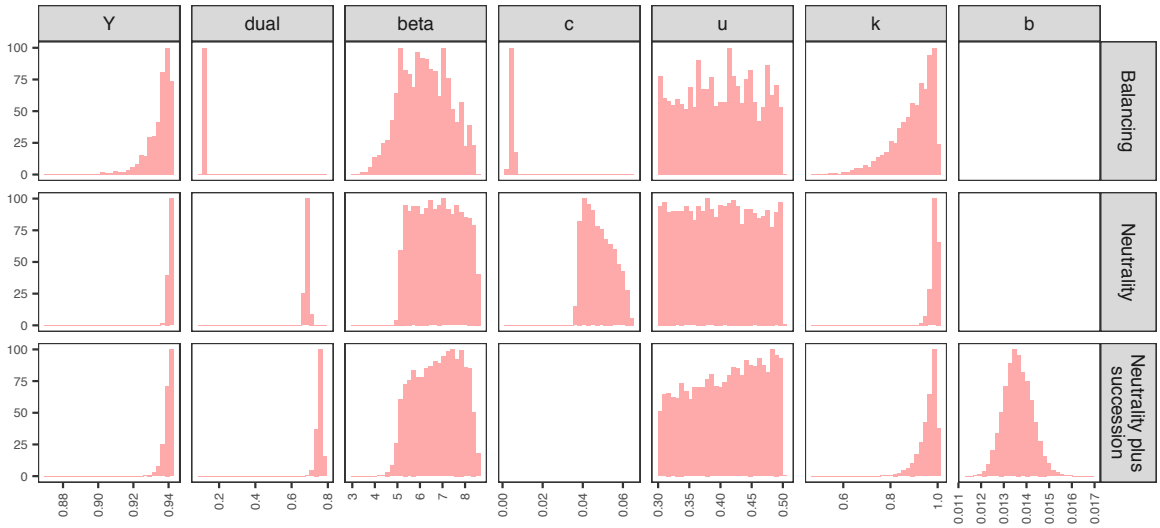

Figure S2 | Posterior distribution for *E. coli* / fluoroquinolones, 2015. See Fig. S1 for details.

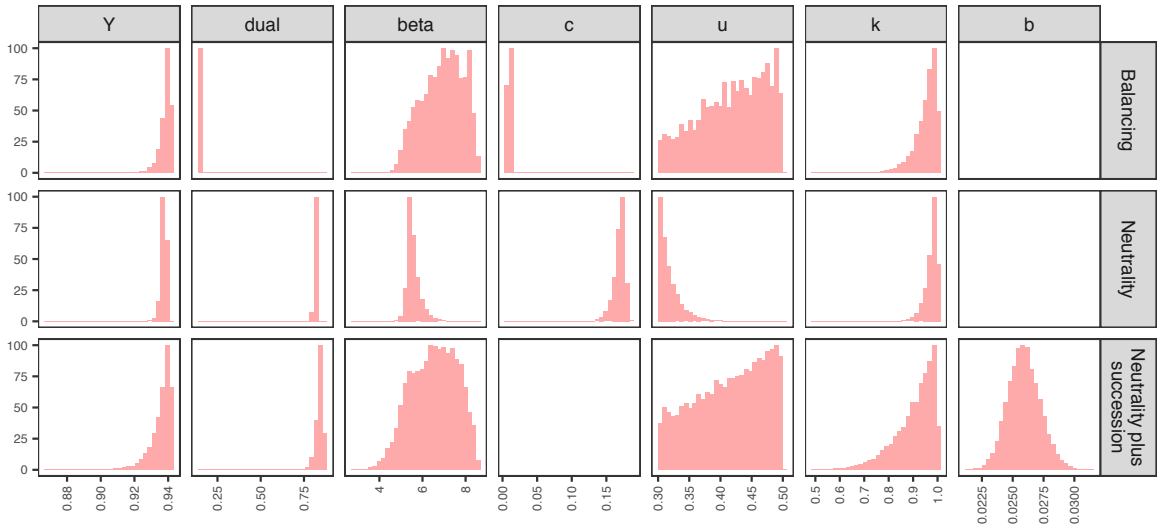

Figure S3 | Posterior distribution for *E. coli* / penicillin, 2015. See Fig. S1 for details.

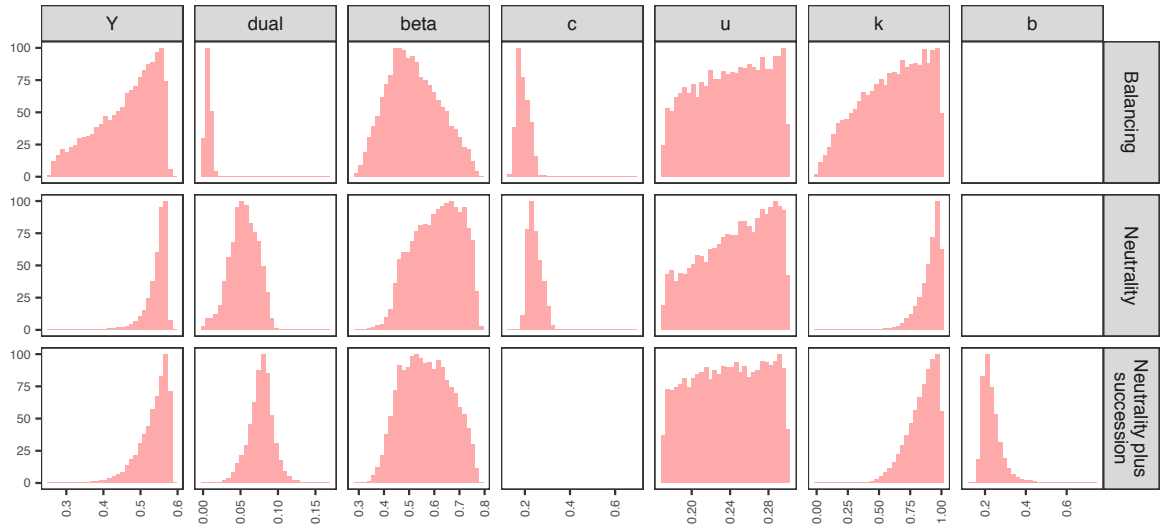

780

781 **Figure S4 |** Posterior distribution for *S. aureus* / meticillin, 2015. See Fig. S1 for

782 details.

783

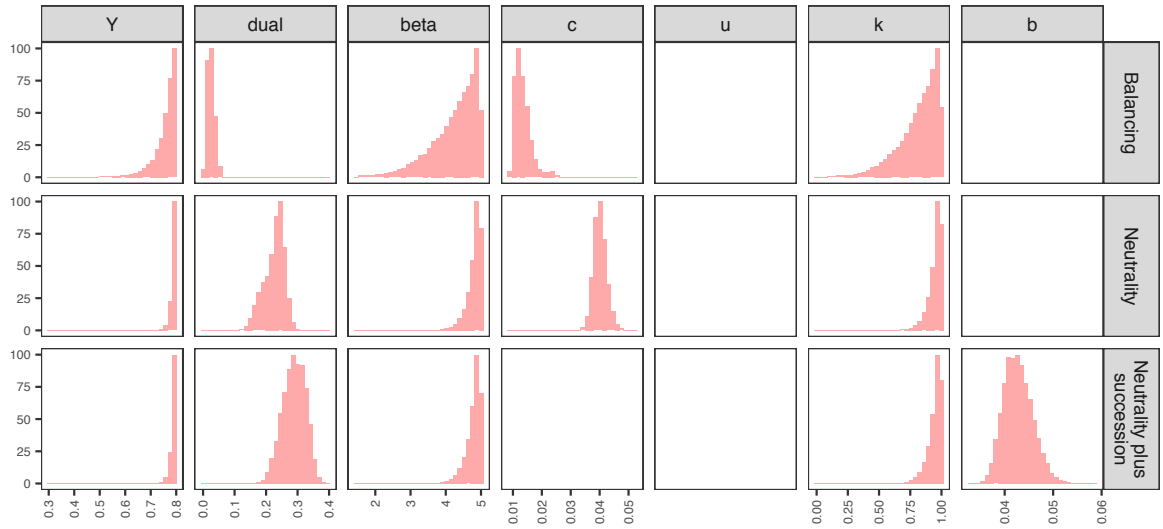

784

785 **Figure S5 |** Posterior distribution for *S. pneumoniae* / macrolides, 2015. See Fig.

786 S1 for details.

787

788 S2. Positive association between carriers: $k > 1$

789

In the main analysis, we assume that k measures relative efficiency of co-colonisation compared to colonisation of an uncolonised host, and hence restrict our attention to $k \leq 1$. However, it is also possible to interpret k as capturing positive association between carriers, as increasing k increases transmission among carriers without impacting upon the overall prevalence of carriage in the population. Thus, it is possible to have $k > 1$ reflecting this mechanism. Allowing for the range $0 \leq k \leq 5$, we find that (a) the fit of the within-host balancing model does not substantially improve and that (b) similar levels of coexistence are possible for the within-host neutral and within-host competition models with lower prevalence of carriage. Here, for illustration, we adopt more restrictive ranges on the prevalence of carriage: $0.2 \leq Y \leq 0.4$ for *S. pneumoniae*, $0.4 \leq Y \leq 0.8$ for *E. coli*, and $0.2 \leq Y \leq 0.4$ for *S. aureus* (**Fig. S6**).

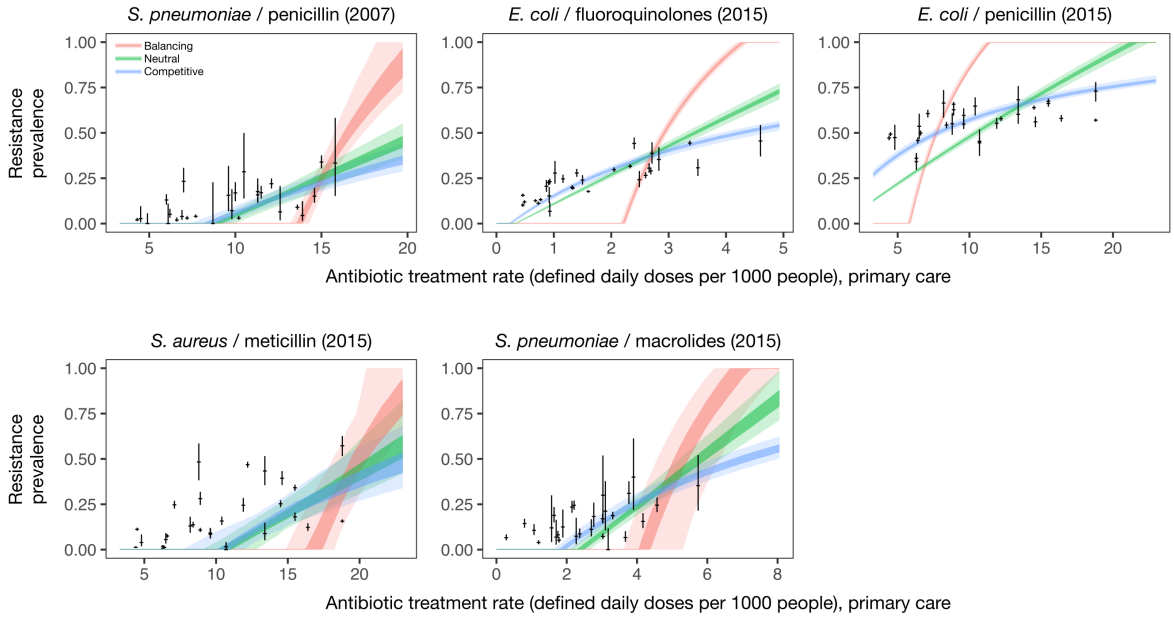

Figure S6 | Model fits with $0 \leq k \leq 5$.

806 *Posterior distributions from model fitting with $0 \leq k \leq 5$*

807

808 Posterior distributions provided in **Figs. S7–S11**.

809

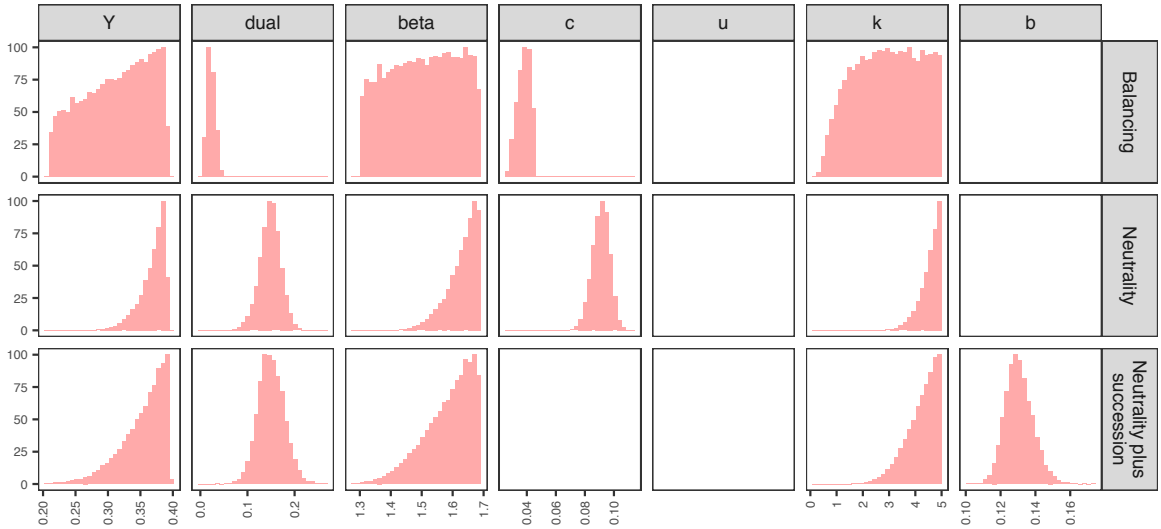

810

811 **Figure S7 |** Posterior distribution for *S. pneumoniae* / penicillin (2007) data set

812 with $0 \leq k \leq 5$.

813

814

815 **Figure S8 |** Posterior distribution for *E. coli* / fluoroquinolones (2015) data set

816 with $0 \leq k \leq 5$.

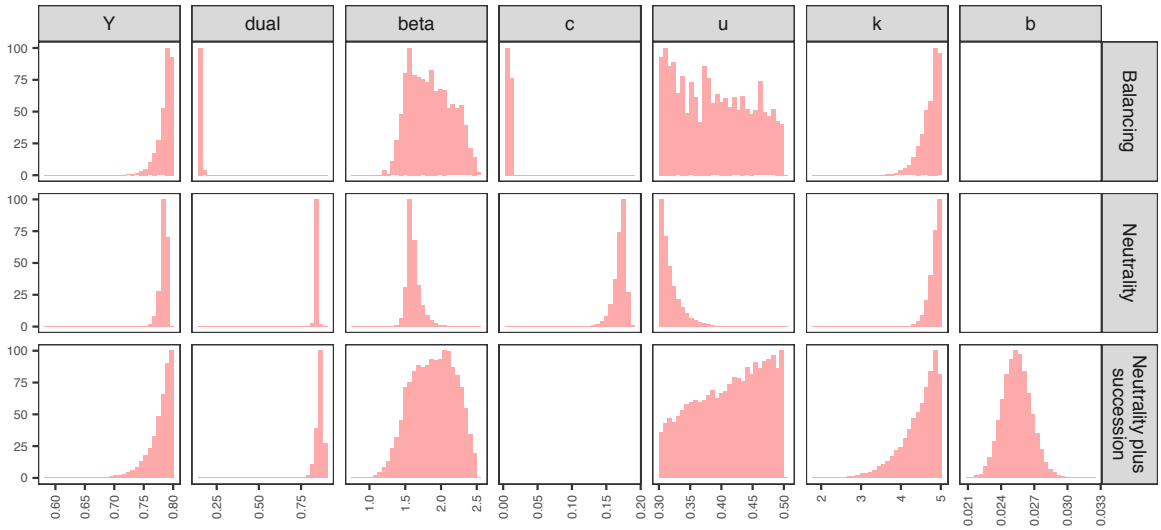

817

818 **Figure S9 |** Posterior distribution for *E. coli* / penicillin (2015) data set with $0 \leq$

819 $k \leq 5$.

820

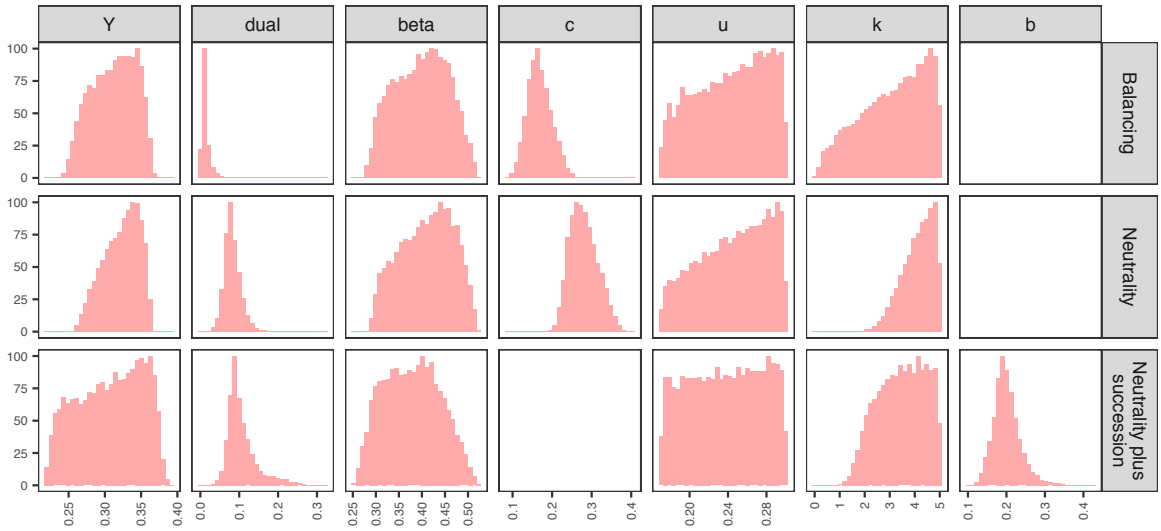

821

822 **Figure S10 |** Posterior distribution for *S. aureus* / meticillin (2015) data set with

823 $0 \leq k \leq 5$.

824

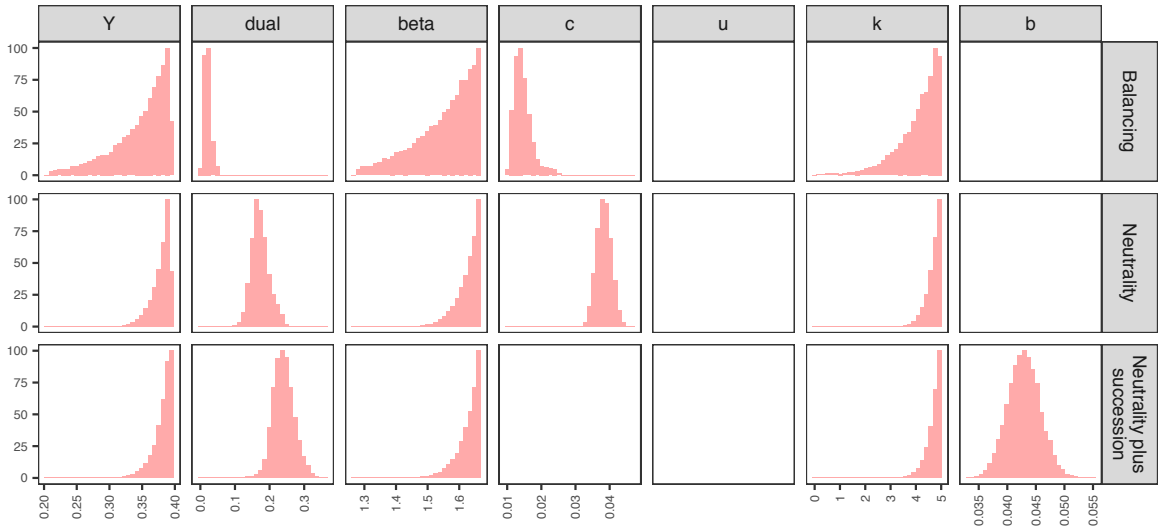

825

826 **Figure S11 |** Posterior distribution for *S. pneumoniae* / macrolides (2015) data

827 set with $0 \leq k \leq 5$.

828

829 *Relative likelihoods from model fitting with $0 \leq k \leq 5$*

830

831 We calculated the relative likelihood for the fitted models, M_i, by comparison of

832 the Akaike Information Criterion (AIC) of each model to that of the best model, M

833 ($\exp[(AIC(M) - AIC(M_i))/2]$) (**Table S2**).

834

Model	**Within-host balancing**	**Within-host neutrality**	**Within-host competition**
S. pneumoniae / penicillin (2007) (n = 3)	4.82×10^{-5}	0.453	1
E. coli / fluoroquinolones (2015) (n = 4)	1.11×10^{-127}	1.03×10^{-12}	1
E. coli / penicillin (2015) (n = 4)	1.12×10^{-161}	1.34×10^{-26}	1

S. aureus / meticillin (2015) (n = 4)	6.87×10^{-4}	0.696	1
S. pneumoniae / macrolides (2015) (n = 3)	3.84×10^{-14}	1.33×10^{-3}	1

Table S2 | Relative likelihoods for model fits with $0 \leq k \leq 5$. The number of parameters, n, is given for each model.

S3. S_R-to-S clearance in within-host competition model

In the within-host neutral model with competition, within-host competition causes R_S carriers to transition into S_R carriers over time. However, an alternative model proposes that the minor complement of resistant cells in S_R carriers may be outcompeted within the host over time, transitioning S_R carriers to S carriers. To verify the robustness of our results against the clearance of resistant cells from S_R carriers, we re-fit the the neutral model with within-host competition to the *S. pneumoniae* / penicillin data set assuming that S_R carriers transition to S carriers at double the rate of the R_S to S_R transition, i.e. $2b$. Adding this transition has a minimal impact on the model fit (**Fig. S12**). The relative likelihood of the model fitted with S_R-to-S clearance is 0.926 compared to the model fitted without S_R-to-S clearance.

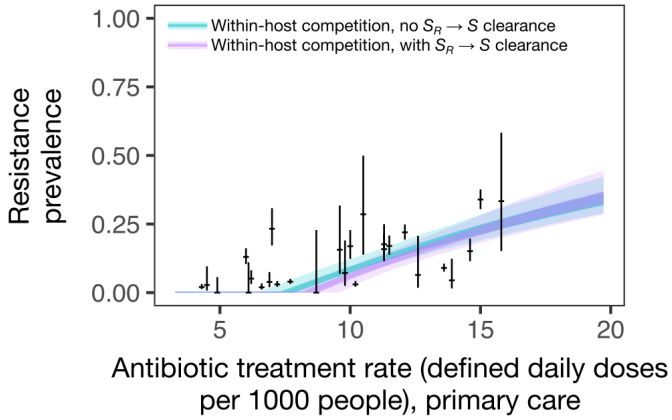

853

854 **Figure S12** | Model fits for *S. pneumoniae* / penicillin (2007) data set without

855 and with S_R-to-S clearance.

856

857 S4. Pneumococcal coexistence without immune memory

858

859 We found that independent clearance of serotypes alone was insufficient to

860 support the high diversity of pneumococcal serotype carriage observed in

861 human populations with only four serotypes maintained (Fig. S13).

862

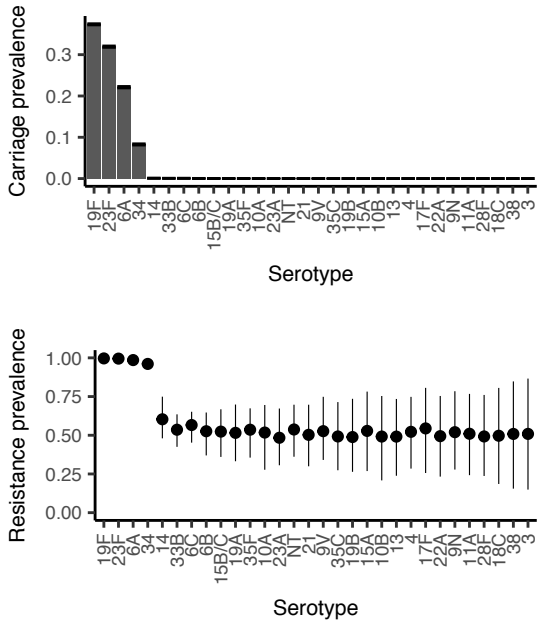

863

Fig. S13 | As serotypes vary greatly in duration of carriage, the mechanism of independent clearance alone is not able to reproduce observed patterns of pneumococcal carriage or resistance prevalence, as all but the four serotypes with the highest duration of carriage are eliminated. Resistance prevalence is close to 50% for eliminated serotypes as stochastic importation of strains (see *Methods*) maintains carriage of both sensitive and resistant strains of each serotype at low prevalence.